



Spencer, J., Lewis, P. A., Takebayashi, Y., Samphire, J. L., Hill, S. A., Hill, N., & Galan, M. C. (Accepted/In press). Green Fluorescent Carbon Dots as Targeting Probes for LED-Dependent Bacterial Killing. *Nano Select*. <https://doi.org/10.1002/nano.202100183>

Publisher's PDF, also known as Version of record

License (if available):  
CC BY

Link to published version (if available):  
[10.1002/nano.202100183](https://doi.org/10.1002/nano.202100183)

[Link to publication record in Explore Bristol Research](#)  
PDF-document

This is the final published version of the article (version of record). It first appeared online via Wiley Open Access at [10.1002/nano.202100183](https://doi.org/10.1002/nano.202100183). Please refer to any applicable terms of use of the publisher.

## University of Bristol - Explore Bristol Research

### General rights

This document is made available in accordance with publisher policies. Please cite only the published version using the reference above. Full terms of use are available: <http://www.bristol.ac.uk/red/research-policy/pure/user-guides/ebr-terms/>

## RESEARCH ARTICLE

# Green fluorescent carbon dots as targeting probes for LED-dependent bacterial killing

Jennifer Samphire<sup>1,2</sup> | Yuiko Takebayashi<sup>2</sup>  | Stephen A. Hill<sup>1</sup> | Nicholas Hill<sup>2</sup> |  
Kate J. Heesom<sup>3</sup> | Philip A. Lewis<sup>3</sup> | Dominic Alibhai<sup>4</sup> | Eilis C. Bragginton<sup>2</sup> |  
Josephine Dorh<sup>5</sup> | Neciah Dorh<sup>5</sup> | James Spencer<sup>2</sup>  | M. Carmen Galan<sup>1</sup> 

<sup>1</sup> School of Chemistry, Cantock's Close, University of Bristol, Bristol, UK

<sup>2</sup> School of Cellular and Molecular Medicine, University of Bristol, Bristol, UK

<sup>3</sup> Proteomics Facility, University of Bristol, Bristol, UK

<sup>4</sup> Wolfson Bioimaging Facility, University of Bristol, Bristol, UK

<sup>5</sup> FluoretiQ Limited, Unit DX, St Philips Central, Bristol, UK

## Correspondence

James Spencer, School of Cellular and Molecular Medicine, University of Bristol, Biomedical Sciences Building, BS8 1QU, Bristol, UK.

Email: [jim.spencer@bristol.ac.uk](mailto:jim.spencer@bristol.ac.uk)

M. Carmen Galan, School of Chemistry, Cantock's Close, University of Bristol, BS8 1TS, Bristol, UK.

Email: [m.c.galan@bristol.ac.uk](mailto:m.c.galan@bristol.ac.uk)

Jennifer Samphire and Yuiko Takebayashi contributed equally

## Funding information

Engineering and Physical Sciences Research Council, Grant/Award Numbers: EP/G036764/1, EP/S026215/1, EP/R043361/1 (TS/R014329/1), EP/T020288/1, L01386X; H2020 European Research Council, Grant/Award Number: COG 648239; EU Cost Action, Grant/Award Number: CA 18132

## Abstract

The emergence of antimicrobial resistance (AMR) represents a significant health and economic challenge worldwide. The slow pace of antibacterial discovery necessitates strategies for optimal use of existing agents, including effective diagnostics able to drive informed prescribing; and development of alternative therapeutic strategies that go beyond traditional small-molecule approaches. Thus, the development of novel probes able to target bacteria for detection and killing, and that can pave the way to effective theranostic strategies, is of great importance. Here we demonstrate that metal-free green-emitting fluorescent carbon dots (FCDs) synthesized from glucosamine-HCl and *m*-phenylenediamine, and featuring 2,5-deoxyfructosazine on a robust amorphous core, can label both Gram-positive (*Staphylococcus aureus*) and Gram-negative (*Escherichia coli*, *Klebsiella pneumoniae*, *Pseudomonas aeruginosa*) bacterial pathogens within 10 minutes of exposure. Moreover, effective killing of Gram-positive and -negative bacteria can be induced by combining FCD treatment with irradiation by LED light in the visible range. Cell-based, electron microscopy and tandem mass tag (TMT) proteomic experiments indicate that FCD administration in combination with LED exposure gives rise to local heating, ROS production, and membrane- and DNA-damage, suggesting multiple routes to FCD-mediated bacterial killing. Our data identify FCDs as materials that combine facile synthesis from low-cost precursors with labeling and light-dependent killing of clinically important bacterial species, and that thus warrant further exploration as the potential bases for novel theranostics.

## KEYWORDS

antimicrobials, bacteria labeling, fluorescent carbon dots, LED-photothermal activation, targeted nano materials

This is an open access article under the terms of the [Creative Commons Attribution](https://creativecommons.org/licenses/by/4.0/) License, which permits use, distribution and reproduction in any medium, provided the original work is properly cited.

© 2021 The Authors. *Nano Select* published by Wiley-VCH GmbH

## 1 | INTRODUCTION

Bacterial infections affect most people at some point in their lives and, while antibiotic treatments exist for most common pathogens, their effectiveness is threatened by growing antimicrobial resistance (AMR). This problem is exacerbated by the rising overuse of broad spectrum antibiotics combined with the slowing development of new antibiotics.<sup>[1]</sup> In an effort to control and prevent growing antibiotic resistance, rapid diagnostic tools that can be used to detect the presence of bacteria are key to avoid antibiotic treatments being unnecessarily prescribed, while use of materials with antimicrobial properties can reduce or prevent infections associated with surfaces or medical devices.<sup>[1b]</sup>

Fluorescent labeling has been previously implemented to investigate antibiotic susceptibility, intracellular pathogenesis and detection of bacterial cell wall proteins.<sup>[2]</sup> However, molecular dyes are usually expensive and predisposed to photobleaching. Fluorescent nanoprobes on the other hand can be designed to exhibit high stability, sensitivity and specificity for their desired target without the limitations of organic fluorophores and fluorescent proteins and thus these nanomaterials have found many applications in the areas of bioimaging, drug delivery and diagnostics.<sup>[3]</sup> Furthermore, the fluorescence properties of molecular fluorophores can be affected upon binding to the target, while intrinsically fluorescent nanoparticles are rarely affected and can be more robust bioimaging tools.<sup>[4]</sup>

One particular class of fluorescent nanoparticles, carbon dots (CDs), have emerged as promising bioimaging probes due to their many advantages over molecular fluorophores and other fluorescent nanoparticles such as the analogous heavy-metal containing quantum dots.<sup>[5]</sup> The synthesis of these water-soluble carbon-based nanodots is often practical and low-cost,<sup>[6]</sup> while CDs tend to be chemically inert, photo-stable and generally non-toxic, making them ideal for biological applications.<sup>[6f,6h,6i,7]</sup> Examples of surface functionalized CDs have been reported to label bacteria with some examples showing bactericidal effects.<sup>[8]</sup> Initial efforts in the field relied on the use of blue-emitting materials which due to the autofluorescence properties of many microorganisms<sup>[9]</sup> overlap with the blue emission of the CDs used, meaning that the sensitivity of such probes was not high enough for practical use and other emission profiles are preferred for this type of applications. In addition, parameters such as nanoparticle type, size, shape and surface functionalization have been shown to have significant effects on targeting ability, intracellular uptake and localization.<sup>[10]</sup>

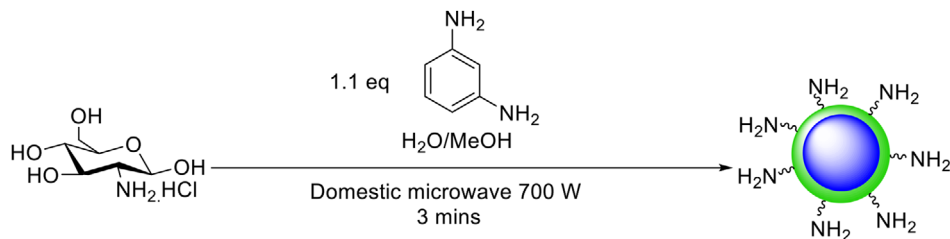
Stemming from our interest in the synthesis of carbon-based water soluble fluorescent probes for bioimaging applications,<sup>[6f,6g,6i]</sup> we recently developed a new class of

green-fluorescent CDs (FCDs) derived from glucosamine and *m*-phenylenediamine (Scheme 1) that could selectively label and kill human cancer cells upon activation by illumination with visible LEDs.<sup>[11]</sup> The unique targeting ability of this nanomaterial was attributed to the presence of 2,5-deoxyfructosazine on the FCD surface. 2,5-deoxyfructosazine is the product of 1,2-aminoaldose self-dimerization during FCD synthesis,<sup>[12]</sup> and analogous fructosazine, is itself a versatile molecule with anti-diabetic and anti-inflammatory properties.<sup>[13]</sup>

Based on these findings, we thus proposed that these green-emitting FCDs could be promising candidates to target live bacteria. Herein, we demonstrate that the unique surface functionality of these green-emitting FCDs can also be used to label both Gram-positive and Gram-negative bacteria. Furthermore, we also show the combination of FCD exposure with LED-activation to exert a bactericidal effect, and investigate the mechanism of bacterial killing action.

## 2 | RESULTS AND DISCUSSION

Green-fluorescent carbon dots (FCDs) surface functionalized with 2,5-deoxyfructosazine were obtained by a three-minute microwave-assisted one-pot reaction of glucosamine and *m*-phenylenediamine following a previously reported synthesis.<sup>[11]</sup> To evaluate the ability of the FCD to label bacteria, different initial FCD concentrations (50–200  $\mu\text{g mL}^{-1}$ ) were incubated with four different bacterial species to assess the optimal labeling conditions over a range of time exposures (10–60 minutes). To that end, *Escherichia coli* (BW25113 strain), a Gram-negative bacterium; and *Staphylococcus aureus* (Newman strain), a Gram-positive bacterium; and further two Gram-negative species, *Pseudomonas aeruginosa* (PA01 strain) and *Klebsiella pneumoniae* (NCTC 5055 strain) were chosen as relevant microorganisms. Labeling of the bacteria was assessed using and confocal microscopy and quantified using a UV-Vis plate reader. To our delight, all bacterial species evaluated showed labeling after as little as 10 minutes incubation with green FCDs (Figure 1B) and at FCD concentrations as low as 25  $\mu\text{g mL}^{-1}$ . As expected, fluorescence labeling increased with the amount of FCDs used. In general, consistent labeling was achieved with a  $1 \times 10^8$  cfu  $\text{mL}^{-1}$  suspension of bacteria in phosphate buffered saline (PBS) incubated with 200  $\mu\text{g mL}^{-1}$  of FCDs at room temperature for 30 minutes. This concentration and exposure time was thus chosen for imaging experiments to ensure homogeneous labeling of the bacterial species. (see ESI Figure S1B and S1C). To quantify bacterial labelling, fluorescence measurements of FCD-labeled bacterial suspensions were compared to a FCD calibration curve. Uniformly, FCDs



**SCHEME 1** General synthetic approach to access green-emitting FCDs

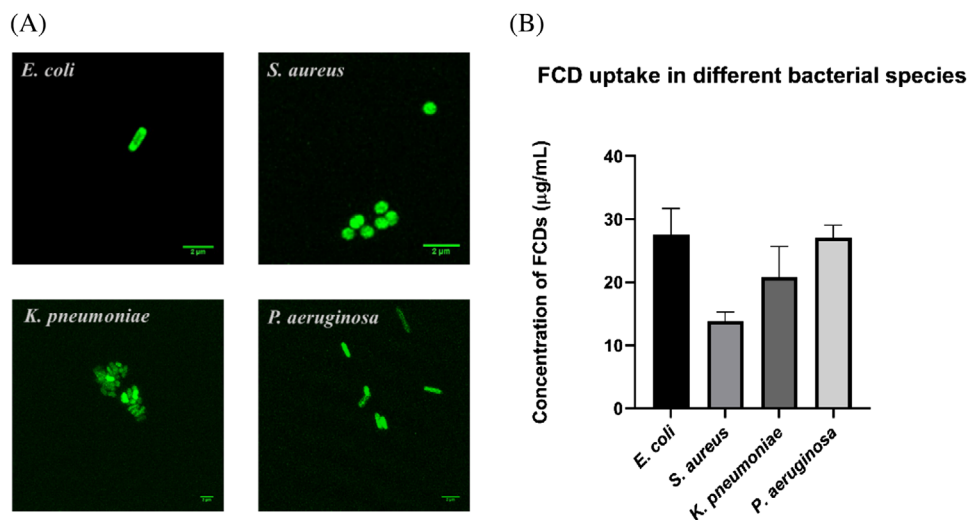


**FIGURE 1** FCDs label Gram-positive and -negative Bacteria. A, Hyvolution confocal microscopy z-stack max-projected images of FCD labelled bacteria after 30 minutes exposure to FCDs; *E. coli*, *S. aureus*, *P. aeruginosa* and *K. pneumoniae* and (B) quantification of FCD labeling for each bacteria species after 10 minutes incubation with  $200 \mu\text{g mL}^{-1}$  of FCDs at room temperature.

were found to show increased labelling of Gram-negative bacteria when compared with the Gram-positive species *S. aureus*, which had the lowest levels of labelling (Figure 1). Gram-negative bacteria have a thin layer of peptidoglycan sandwiched between two membranes whereas Gram-positive bacteria have just one membrane surrounded by a thicker layer of peptidoglycan, and moreover possess a stronger overall negative charge due to the presence of wall teichoic acids.<sup>[14]</sup> These differences in cell wall composition affect the interactions of bacteria with external stimuli and their sensitivity to antibacterial agents. Our results thus suggest that interactions with FCDs are likely to differ between the two different types of bacterial cell walls.

Previous investigations of the chemical structure of the green-emitting FCDs<sup>[11]</sup> revealed that the carbon-based probe contains a stable amorphous core, decorated with 2,5-deoxyfructosazine as the major surface component (See Figure S1A in supporting information for FCD fluorescence emission spectra). It is however important to note that neither previously reported amine coated blue-emitting FCDs<sup>[6i]</sup> or 2,5-deoxyfructosazine (itself non-fluorescent) isolated from green FCDs or from a commer-

cial source, were able to fluorescently label the bacteria, demonstrating that the observed effects can be attributed to the properties of the green-emitting FCDs as a whole (see Figures S2A and 2B in ESI).

To establish whether the FCDs are internalized within the bacteria, or remain associated with the cell surface, FCD-treated bacteria were then labelled with the membrane dye FM 4-64FX (Figure 2). FM 4-64FX is a lipophilic probe which has low fluorescence in aqueous media, but upon binding to plasma membranes fluoresces intensely in the infrared, allowing visualization of the bacterial membrane and hence localization of the green-emitting FCDs with respect to this.<sup>[15]</sup> Confocal microscopy images of bacteria labeled with both FCDs (green) and FM 4-64FX (red, Figure 2) identified distinct patterns of staining for the two labels, confirmed that the FCDs are internalized within the bacteria and hence demonstrating their ability to penetrate the bacterial envelope.

Having confirmed that FCDs are internalized by bacteria, the toxicity of the green FCDs towards both the Gram-negative (*E. coli*, *K. pneumoniae*, *P. aeruginosa*) and Gram-positive (*S. aureus*) was next explored. Overall, little

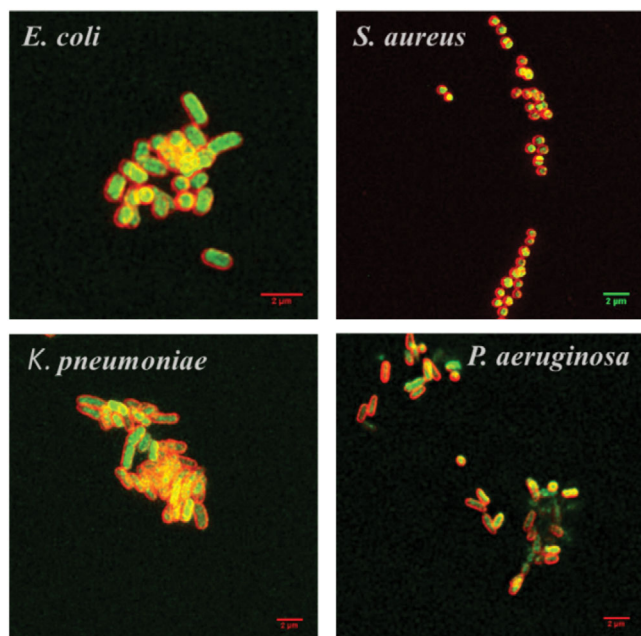


**FIGURE 2** FCDs are internalised by Gram-positive and -negative bacteria. Confocal image of different bacterial species incubated with membrane dye FM 4-64FX (red) and FCDs (green) for 30 minutes

antibacterial activity was detected upon treatment with FCDs, even at high FCD concentrations ( $\text{MIC} > 1024 \mu\text{g mL}^{-1}$ ), with the most notable effect being an increase in the duration of the lag phase of bacterial growth (see ESI).

Previously, we have shown photothermal activation of green-emitting FCDs using low cost blue-light-emitting diodes (LEDs,  $\lambda_{\text{em}} = 460 \text{ nm}$ ).<sup>[11]</sup> Irradiation by blue LEDs in the absence of FCDs did not induce toxic effects on bacteria, however, when LED irradiation was combined with FCD exposure, bactericidal activity was detected towards all four species tested (*E. coli*, *S. aureus*, *K. pneumoniae* and *P. aeruginosa* (ESI, Figure S4)). Complete killing was reproducibly observed after treatment with  $200 \mu\text{g/mL}$  FCDs with 4 hours of irradiation, and significant killing ( $> 95\%$ ) could be observed after just 90 minutes of LED irradiation (see data for *E. coli* and *S. aureus* in Figure 3A).

For two strains of *E. coli*, the antimicrobial effects of UV-B irradiation have been shown to be potentiated by fructosazine.<sup>[16]</sup> To demonstrate that the bactericidal effects observed here were linked to the combination of FCD/LED treatment, and not due to either the presence of 2,5-deoxyfructosazine/LED, or 2,5-deoxyfructosazine alone, *E. coli* was treated with 2,5-deoxyfructosazine obtained from a commercial source at the same concentrations as those found on the FCDs, as estimated by NMR, and also exposed to LED irradiation under the same conditions as previously used (See ESI figures S2B and S5 for details). Viable counts of treated cells showed that signifi-

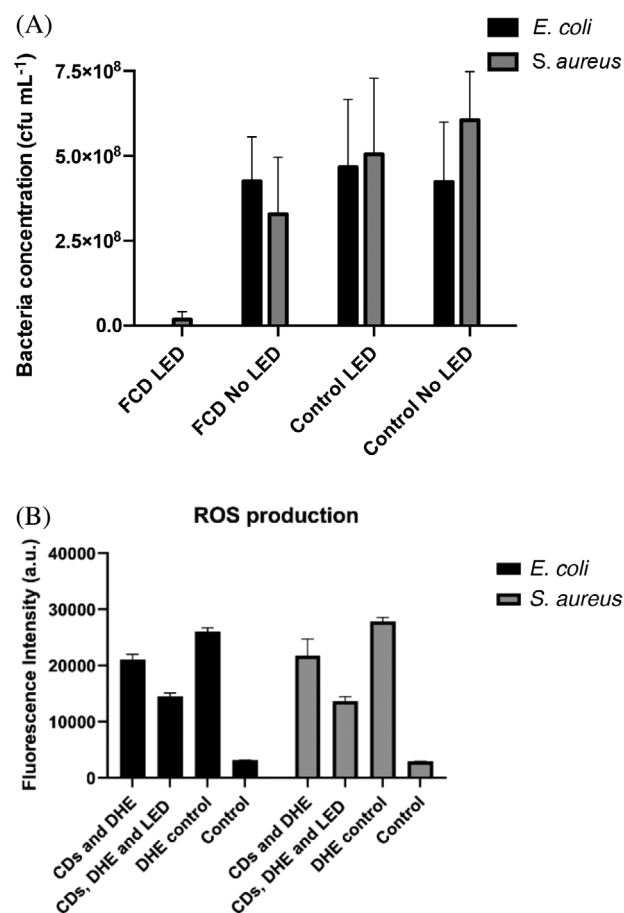


**FIGURE 3** A, Antimicrobial effects of combined FCD treatment and LED illumination. Viable count shown as  $\text{cfu mL}^{-1}$  of *E. coli* or *S. Aureus* cells treated with green FCDs ( $200 \mu\text{g mL}^{-1}$ ), and controls with and without 90 minutes LED irradiation. Counts were averaged and shown with SD error bars ( $n = 6$ ). B, FCD Treatment and LED Illumination elicits ROS production in Gram-positive and -negative bacteria. Fluorescence intensity measurements show decrease in fluorescence at 460 nm (DHE emission) for *E. coli* and *S. aureus* incubated with  $200 \mu\text{g mL}^{-1}$  FCDs and illuminated with LEDs (FCD, DHE, LED) or kept in the dark (FCD, DHE) for 90 minutes. Fluorescence intensities were averaged and shown with SD error bars ( $n = 3$ )

cant antibacterial effect could only be detected on exposure to the FCD/LED combination ( $t$ -test,  $p < 0.0001$ ), with no effects observed, compared to controls, for cells treated with 2,5-deoxyfructosazine, either with or without LED illumination ( $t$ -test,  $p = 0.4254$  and  $p = 0.3916$  respectively).

Photothermal therapy (PTT) is a promising non-invasive therapeutic strategy, in which nanoparticles embedded within a pathogenic target generate heat, typically in response to exogenously applied light, for thermal ablation. Our previous study of green FCD interactions with cultured human cells<sup>[11]</sup> demonstrated killing to be predominantly mediated by photothermal effects. Accordingly, the temperatures of bacterial suspensions

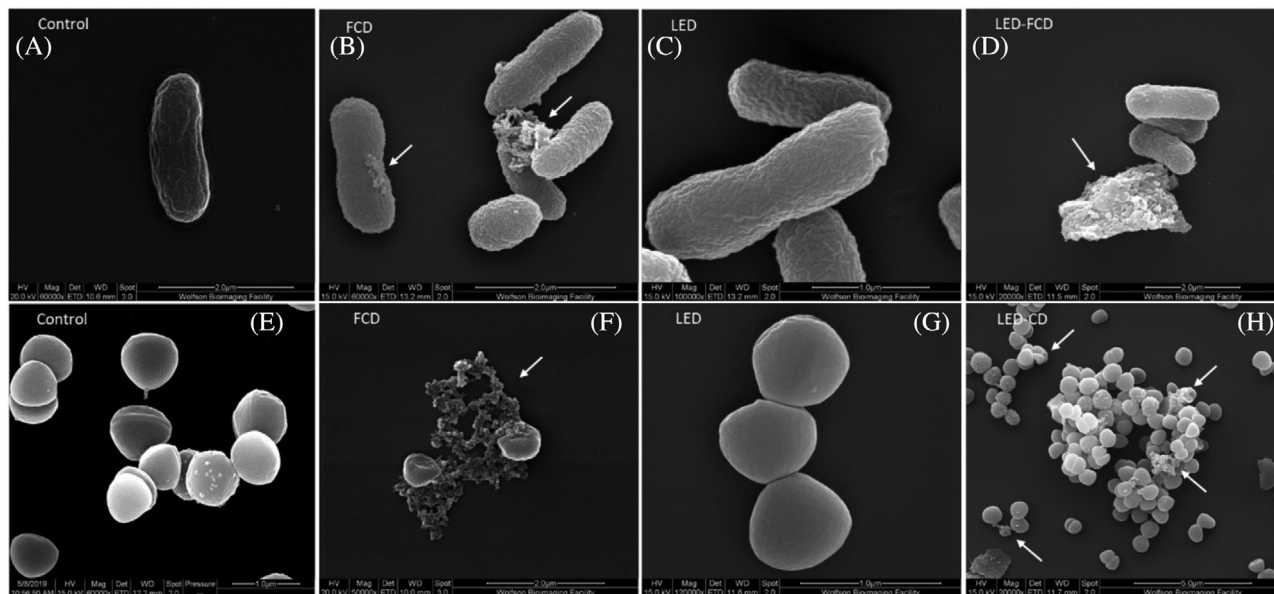


**FIGURE 4** Representative SEM images of *E. coli* (A–D) and *S. aureus* (E–H) with FCD, LED and LED-FCD treatments. Signs of envelope stress/damage are highlighted by arrows

incubated with 200 and 800  $\mu\text{g mL}^{-1}$  FCDs and exposed to LED irradiated for 60 minutes were measured, and found to be 3°C higher (32°C and 33°C respectively) than those of cultures exposed to LED irradiation only, that is, in the absence of FCDs.<sup>[17]</sup> These data suggest that, consistent with our earlier investigation, photothermal activation of FCDs internalized within the bacteria might be responsible for at least some portion of the observed antimicrobial activity. However, we also sought to identify whether other mechanisms might contribute to the effects of FCD exposure upon bacteria. Reactive oxygen species (ROS) production is involved in the mechanism of action of multiple physical and chemical antibacterial agents and treatments.<sup>[18]</sup> Moreover, it has been shown that FCDs can produce ROS upon photoexcitation owing to the band-edge defect effect and that the photosensitization performance of FCDs is also dependent on the surface functionalization and irradiation source.<sup>[19]</sup> Thus the superoxide indicator dihydroethidium (DHE, for which a decrease in fluorescence on oxidation indicates ROS production) was used to monitor ROS formation in LED and FCD treated bacteria. For both *E. coli* and *S. aureus* the fluorescence intensity of DHE for FCD-incubated (200  $\mu\text{g/mL}$ ) bacteria after 90 minutes of LED illumination was significantly lower (by 46% compared to DHE controls) than that of cultures treated with FCDs but in the absence of LED illumination (*t*-test  $p = 0.0007$  and  $p = 0.0008$  respectively) (Figure 3B). This suggests that FCDs, when combined with LED irradiation, are eliciting ROS generation. Taken together, these data indicate that stress factors, such as ROS and temperature changes, are

likely pertinent to the observed toxicity engendered by the LED/FCD combination.

Confocal microscopy (Figure 2) helped us demonstrate the ability of FCDs to penetrate the envelopes of both Gram-positive and -negative bacteria. To establish whether FCD exposure leads to membrane damage, and investigate the possibility that this may also contribute to the observed effects upon bacterial growth, scanning electron microscopy (SEM) was used to study the effects of LED and FCD exposure on *E. coli* and *S. aureus*. Bacterial cells exposed to 512  $\mu\text{g mL}^{-1}$  FCDs, either with or without LED irradiation, indeed showed signs of envelope stress, evident in increased membrane blebbing and lysis. Importantly, LED irradiation alone did not induce these phenotypes, with these samples comparable to the control cells (Figure 4).

To further probe the cellular stress responses activated by FCD exposure, and the effects upon this of LED irradiation, *E. coli* and *S. aureus* cultures were grown in M9 minimal media in the presence or absence of 512  $\mu\text{g mL}^{-1}$  FCDs and with and without LED irradiation, and analyzed by tandem mass tag (TMT) proteomics. Approximately 2600 individual protein hits were obtained in each of the bacterial cultures analyzed. From each sample (LED irradiated, FCD-treated or FCD-treated and LED irradiated), the total protein hits were compared against the control untreated sample. Changes in protein expression levels are summarized in Figure 5. The functions of proteins of interest were searched using PantherDB<sup>44</sup>.

In both bacterial species of the tested conditions, LED irradiation had the least effect on protein expression levels

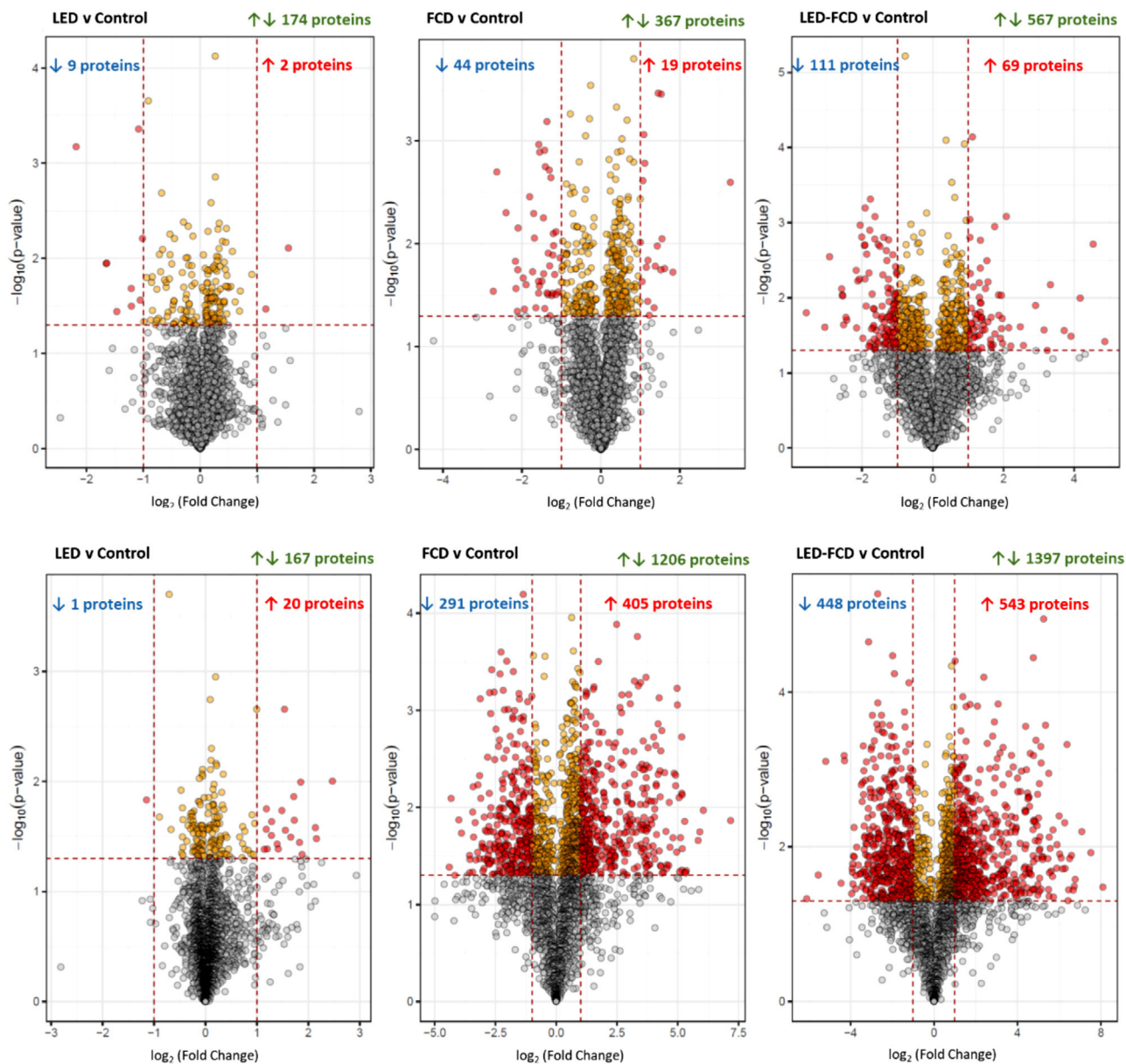


**FIGURE 5** Volcano plots of (Top) *E. coli* and (Bottom) *S. aureus* treated with LED, FCD and LED-FCD. Overall number of proteins with changes in abundance levels indicated in green font. Grey circles represent proteins with differences in abundance levels (compared with control) that are not statistically significant, yellow circles represent those with statistical significance ( $p < 0.05$ ) and red circles represent those that are  $\geq 2$ -fold different in abundance

(174 *E. coli* and 167 *S. aureus* proteins were identified as up- or down-regulated,  $p < 0.05$ ). Only 11 and 21 proteins in the two species, respectively, showed over 2-fold changes in expression level compared with the control. In *E. coli*, upregulated proteins included cation efflux protein (CusF), acetolactate synthetase (IlvG) and RNA helicase (DeaD), while various protein and amino acid transport proteins, such as the inner membrane metabolite transport protein YhjE and the Sec-independent protein translocase protein TatE, were downregulated. In *S. aureus*, 20 proteins were upregulated, including the amino acyl tRNA synthetases ValS and PheT, and only 1 protein, the elon-

gation factor Tu fragment Tuf was downregulated by over 2-fold compared to the control. All proteins of interest are summarized in Figure 6 and the complete list of proteins with  $\geq 2$ -fold changes in expression level is provided in the ESI.

Upon FCD exposure, the number of protein expression changes doubled in *E. coli* and increased by 7-fold in *S. aureus*. In *E. coli*, the protein showing the highest increase in expression level was D-galactonate dehydratase (DgoD), followed by a range of proteins involved in cellular and metabolic processes, some of which were indicative of DNA damage (UvrA, RecN), cell envelope stress (YmgD,





responses to both membrane and DNA damage. In the case of *S. aureus*, the effect of FCD exposure upon the proteome is more profound, but also includes proteins involved in the response to ROS exposure. However, when FCD treatment is augmented with LED irradiation, in both organisms proteomic signatures are consistent with a response to multiple stressors that include both membrane and DNA damage, as well as elevated ROS-levels.

### 3 | CONCLUSIONS

In summary, we have shown that green-emitting FCDs can be used to label both Gram-positive and Gram-negative bacteria within minutes of exposure at room temperature. Moreover, combining FCD treatment with LED-activation leads to effective bacteria cell killing. There are very few examples of FCD photothermal activation in antimicrobial PTT<sup>[21]</sup> and most materials contain transition metals which can be activated with NIR light or other sensitizers for photodynamic therapy applications or do not achieve complete bacteria killing.<sup>[22]</sup> We showed that the targeting properties exhibited by the FCDs are dependent upon the surface functionality on the nanomaterial, with the presence of 2,5-deoxyfructosazine on the FCD surface being key, and that the FCDs are internalized within the bacterial cell. Our investigations of the mechanism of bactericidal action suggest that upon FCD exposure, both *E. coli* and *S. aureus* experience membrane and DNA damage, as evidenced by both SEM and proteomic experiments, while combination of the FCD exposure with mild LED irradiation enhances DNA damage and induces additional effects including ROS production and local heating. In summary, our data show that these low cost metal-free bifunctional nanoprobe display unique physico-chemical and targeting properties that can be exploited as bioimaging tools, as well as in antimicrobial PTT and hence show great potential for further development as effective theranostic agents with potential application in devices for bacterial detection and/or incorporation in surfaces and materials with antimicrobial properties.

### 4 | MATERIALS AND METHODS

#### 4.1 | Bacterial strains, media, growth conditions, suspensions and blue-LED irradiation

*Escherichia coli* BW 25113, *K. pneumoniae* NCTC 5055, *P. aeruginosa* PA01 and *S. aureus* Newman were used in this study. All four strains were grown on Nutrient agar/broth (Neogen) at 37°C overnight (18–20 hours) unless other-

wise stated. Bacterial suspensions were prepared from overnight plates in PBS to an OD600 of 0.8–1.0 ( $\sim 1 \times 10^9$  cfu mL<sup>-1</sup>) unless otherwise stated. LED-irradiated samples were exposed to blue-LED strip lights (24 W, 12 V,  $\lambda_{em} = 460$  nm) for durations specified below. The power density of the LED was 55 mW cm<sup>-2</sup> (Blue-LED strips purchased from Amazon were arranged to cover an area of 23 × 19 cm on a 41.5 × 29.5 cm board)

#### 4.2 | FCD preparation

FCDs were prepared as previously described.<sup>[11]</sup> Briefly, glucosamine-HCl and *m*-phenylenediamine were heated for 3 minutes in a domestic microwave (800W), re-suspended in water and filtered through a MWCO 10 kDa centrifugal concentrator. The solution was then reduced in vacuo and hydrolyzed in water prior to use.

#### 4.3 | Sample preparation for confocal imaging

10  $\mu$ L of 5 mg mL<sup>-1</sup> FCDs were added to 240  $\mu$ L bacterial suspensions to a final concentration of 200  $\mu$ g mL<sup>-1</sup>. The mixtures were rotated for 30 minutes at room temperature before centrifuging at 5000  $\times g$  for 5 minutes. The supernatants were removed and the cell pellets re-suspended in 25  $\mu$ L 2% paraformaldehyde (PFA). The cells were left to fix for 1 hour at room temperature before transferring 5  $\mu$ L into 15  $\mu$ L ProLong<sup>TM</sup> Gold Antifade mountant (ThermoFisher). For cell membrane staining, FCDs were added to bacterial suspensions to a final concentration of 40  $\mu$ g mL<sup>-1</sup> and processed as above. Prior to the addition of PFA, the cell pellets were washed in PBS solution, re-suspended in 25  $\mu$ L of 100  $\mu$ g mL<sup>-1</sup> of FM 4–64FX (ThermoFisher) and shaken at 37°C for 30 minutes. 10  $\mu$ L of 4% PFA was then added and processed as above. The samples were mounted on glass slides with coverslips and left to set at room temperature for at least 12 hours.

#### 4.4 | HyVolution confocal microscopy

Images were acquired on a Leica TCS SP8 system attached to a Leica DMI8 inverted microscope (Leica Microsystems) using a 100x HC PL APO CS2 oil immersion objective. The FCD-treated samples were excited using a 120 mW 405 nm diode laser. Fluorescence of the FCDs were detected using a hybrid detector operating over an emission range of 480–550 nm and images acquired at 512 × 512 pixels. FM 4–64FX (ThermoFisher)-treated samples were excited using a white light laser tuned to 561 nm and

fluorescence detected over an emission range of 700–770 nm.

#### 4.5 | Growth curves

5 milliliter overnight bacterial cultures were centrifuged at 2900 xg for 10 minutes at room temperature and washed twice in PBS. Serial dilutions of FCDs in water were prepared in flat-bottom 96-well plates (Corning), inoculated with 10  $\mu\text{L}$  of  $1 \times 10^8$  cfu  $\text{mL}^{-1}$  HyVolution Confocal microscopy of washed cells and continuously shaken on a rotating platform with or without blue-LED exposure for up to 4 hours. The samples were then further diluted 10-fold in Mueller Hinton broth 2 (Sigma-Aldrich) and placed in a plate reader (BMG Omega) for absorbance readings at 600 nm every 10 minutes for 16.5 hours at 37°C.

#### 4.6 | Viable cell counting

Sample preparation was as described for confocal imaging above. After 30 minutes exposure to FCDs, samples were irradiated with LED lights for 30, 60 or 90 minutes. The LED source was placed 5 cm away from the cultures.

The samples were then centrifuged at 5000 xg for 10 minutes and the cell pellet resuspended in 1 mL of PBS. 25  $\mu\text{L}$  of this suspension was taken and diluted in ten-fold serial dilutions up to  $10^{-7}$ . 100  $\mu\text{L}$  of the last three dilutions were plated on to agar plates and incubated overnight. Cell colonies were then counted to determine viable cell counts.

#### 4.7 | Temperature measurements

In a flat-bottom 96-well plate (Corning), 240  $\mu\text{L}$  of bacterial suspensions were mixed with either 10  $\mu\text{L}$  (800  $\mu\text{g mL}^{-1}$  final concentration) or 2  $\mu\text{L}$  (200  $\mu\text{g mL}^{-1}$ ) of 20 mg  $\text{mL}^{-1}$  FCDs. Control wells contained PBS only. Wells were either irradiated with LEDs or kept in the dark, temperature was recorded at regular 30 minutes intervals. A Thermocouple (type K from Fisher Scientific) was used to record temperature to 1 decimal place.

#### 4.8 | Dihydroethidium ROS determination

192  $\mu\text{L}$  of bacterial suspensions were added to wells of two flat-bottom 96 well plates. Eight microlitre of either FCDs (10 mg  $\text{mL}^{-1}$ ) or sterile water was incubated for 1 hour. One plate was then irradiated with LED lights for 90 minutes whilst the other was kept in the dark. Ten microlitre dihydroethidium (DHE) (1 mg  $\text{mL}^{-1}$ ) was then added to

each well and fluorescence measured at  $\lambda_{\text{ex}} = 350$  nm and  $\lambda_{\text{em}} = 460$  nm (BMG PolarStar Omega plate reader).

#### 4.9 | SEM

One milliliter bacterial overnight cultures were centrifuged at 13,000 xg for 5 minutes and the pellets washed once in PBS. FCDs were added to yield a final concentration of 512  $\mu\text{g mL}^{-1}$  and incubated for 30 minutes with rotation. After 30 minutes, the blue-LED board was placed in front of the rotator and samples not requiring LED-treatment were covered with foil. The samples were rotated for another 30 minutes before centrifuging at 8000 xg for 5 minutes and washing twice in PBS. On the last wash, 50  $\mu\text{L}$  of sample was removed, centrifuged and the pellet resuspended in 50  $\mu\text{L}$  of PBS. Samples were fixed on poly-L-lysine (0.1% w/v in water) treated glass coverslips in 2.5% glutaraldehyde overnight at 4°C. The samples were dehydrated in a series of ethanol solutions from 20, 50, 70, 90 and 100% and chemically dried with hexamethyldisilazane (HMDS) before being mounted on metal stubs and gold sputter coated (Emitech). The samples were imaged at magnifications of 20,000–120,000x on the FEI Quanta 200 FEG-SEM with a working distance of 10–13 mm, chamber pressure of  $< 10^{-5}$  Pa in high vacuum mode and an accelerating voltage of 15–10 kV.

#### 4.10 | Proteomics sample preparation and analysis

##### 4.10.1 | TMT labeling and high pH reversed-phase chromatography

Whole cell lysates were obtained from *E. coli* and *S. aureus* cultures grown in M9 minimal media in duplicate for 6 and 3 hours respectively, with or without 512  $\mu\text{g mL}^{-1}$  FCD and continuous LED irradiation. The proteomics cultures were grown 10 cm away from the LED source. Aliquots of 50  $\mu\text{g}$  of each sample were digested with trypsin (2.5  $\mu\text{g}$  trypsin per 100  $\mu\text{g}$  protein; 37°C, overnight), labeled with TMT ten plex reagents according to the manufacturer's protocol (Thermo Fisher Scientific) and the labeled samples pooled.

The pooled sample was evaporated to dryness, resuspended in 5% formic acid and then desalted using a Sep-Pak cartridge according to the manufacturer's instructions (Waters, Milford, Massachusetts, USA). Eluate from the SepPak cartridge was again evaporated to dryness and resuspended in buffer A (20 mM ammonium hydroxide, pH 10) prior to fractionation by high pH reversed-phase chromatography using an Ultimate 3000 liquid chromatography system (Thermo Scientific). In brief, the

sample was loaded onto an XBridge BEH C18 Column (130Å, 3.5 µm, 2.1 mm × 150 mm, Waters, UK) in buffer A and peptides eluted with an increasing gradient of buffer B (20 mM Ammonium Hydroxide in acetonitrile, pH 10) from 0–95% over 60 minutes. The resulting fractions were evaporated to dryness and resuspended in 1% formic acid prior to analysis by nano-LC MSMS using an Orbitrap Fusion Lumos mass spectrometer (Thermo Scientific).

#### 4.10.2 | Nano-LC mass spectrometry

High pH RP fractions were further fractionated using an Ultimate 3000 nano-LC system in line with an Orbitrap Fusion Lumos mass spectrometer (Thermo Scientific). In brief, peptides in 1% (vol/vol) formic acid were injected onto an Acclaim PepMap C18 nano-trap column (Thermo Scientific). After washing with 0.5% (vol/vol) acetonitrile 0.1% (vol/vol) formic acid peptides were resolved on a 250 mm × 75 µm Acclaim PepMap C18 reverse phase analytical column (Thermo Scientific) over a 150 minutes acetonitrile gradient, divided into seven gradient segments (1–6% solvent B over 1 minute, 6–15% B over 58 minutes, 15–32% B over 58 minutes, 32–40% B over 5 minutes, 40–90% B over 1 minute, held at 90% B for 6 minutes and then reduced to 1% B over 1 minute) with a flow rate of 300 nl min<sup>-1</sup>. Solvent A was 0.1% formic acid and Solvent B was aqueous 80% acetonitrile in 0.1% formic acid. Peptides were ionized by nano-electrospray ionization at 2.0 kV using a stainless steel emitter with an internal diameter of 30 µm (Thermo Scientific) and a capillary temperature of 275°C.

All spectra were acquired using an Orbitrap Fusion Lumos mass spectrometer controlled by Xcalibur 3.0 software (Thermo Scientific) and operated in data-dependent acquisition mode using an SPS-MS3 workflow. FTMS1 spectra were collected at a resolution of 120,000, with an automatic gain control (AGC) target of 200,000 and a max injection time of 50 ms. Precursors were filtered with an intensity threshold of 5000, according to charge state (to include charge states 2–7) and with monoisotopic peak determination set to Peptide. Previously interrogated precursors were excluded using a dynamic window (60 seconds +/- 10 ppm). The MS2 precursors were isolated with a quadrupole isolation window of 0.7 m/z. ITMS2 spectra were collected with an AGC target of 10,000, max injection time of 70 ms and CID collision energy of 35%.

For FTMS3 analysis, the Orbitrap was operated at 50,000 resolution with an AGC target of 50,000 and a max injection time of 105 ms. Precursors were fragmented by high energy collision dissociation (HCD) at a normalized collision energy of 60% to ensure maximal TMT reporter ion yield. Synchronous precursor selection (SPS) was enabled to include up to 5 MS2 fragment ions in the FTMS3 scan.

#### 4.10.3 | Data analysis

The raw data files were processed and quantified using Proteome Discoverer software v2.1 (Thermo Scientific) and searched against the UniProt *E. coli* strain K12 database (4469 sequences downloaded February 2019) or *S. aureus* strain Newman database (2583 sequences downloaded December 2019) using the SEQUEST algorithm.<sup>[23]</sup> Peptide precursor mass tolerance was set at 1 ppm, and MS/MS tolerance was set at 0. Da. Search criteria included oxidation of methionine (+15.9949) as a variable modification and carbamidomethylation of cysteine (+57.0214) and the addition of the TMT mass tag (+229.163) to peptide N-termini and lysine as fixed modifications. Searches were performed with full tryptic digestion and a maximum of two missed cleavages were allowed. The reverse database search option was enabled and all data were filtered to satisfy a false discovery rate (FDR) of 5%.

Volcano plots were plotted to visualize statistical significance (p-value) versus fold change using R studio.<sup>[24]</sup> PantherDB was used for geneontology analysis.<sup>[25]</sup>

#### ACKNOWLEDGMENTS

This research was supported by ERC-COG: 648239 (MCG), EPSRC EP/G036764/1 (JSamphere) and EPSRC EP/S026215/1 (MCG, JS). EP/R043361/1 (TS/R014329/1) (MCG, JS, ND) and GCRF EP/T020288/1 (MCG, JS). The authors would like to thank the following members of the Wolfson Bioimaging Facility for their assistance: Chris Neal and Judith Mantell for the SEM work and Alan Leard for the confocal microscopy work and BrisSynBio, a BBSRC/EPSRC-funded Synthetic Biology Research Centre (L01386X) for funding the Hyvolution system. This publication has risen from discussion at COST Action GLYCONanoPROBES (CA18132), supported by COST (European Cooperation in Science and Technology).


#### DATA AVAILABILITY STATEMENT

The data that supports the findings of this study are available in the supplementary material of this article.

#### ORCID

Yuiko Takebayashi  <https://orcid.org/0000-0002-6224-0224>

James Spencer  <https://orcid.org/0000-0002-4602-0571>

M. Carmen Galan  <https://orcid.org/0000-0001-7307-2871>

#### REFERENCES

1. R. Aminov, *Biochem. Pharmacol.* **2017**, *133*, 4.
2. a) B. L. Roth, M. Poot, S. T. Yue, P. J. Millard, *Appl. Environ. Microbiol.* **1997**, *63*, 2421; b) D. A. Drevets, A. M. Elliott, *J. Immunol. Methods* **1995**, *187*, 69; c) C. Anaya, N. Church, J. P. Lewis, *Proteomics* **2007**, *7*, 215.

3. a) H. Zhu, J. L. Fan, J. J. Du, X. J. Peng, *Acc. Chem. Res.* **2016**, *49*, 2115; b) Y. H. Chan, P. J. Wu, *Part Part Syst. Char.* **2015**, *32*, 11; c) S. M. Janib, A. S. Moses, J. A. MacKay, *Adv. Drug Deliv. Rev.* **2010**, *62*, 1052; d) J. Xie, S. Lee, X. Chen, *Adv. Drug Deliv. Rev.* **2010**, *62*, 1064; e) M. A. Hahn, A. K. Singh, P. Sharma, S. C. Brown, B. M. Moudgil, *Anal. Bioanal. Chem.* **2011**, *399*, 3.
4. O. S. Wolfbeis, *Chem. Soc. Rev.* **2015**, *44*, 4743.
5. a) Z. Zhu, Q. Li, P. Li, X. Xun, L. Zheng, D. Ning, M. Su, *PLoS One* **2019**, *14*, e0216230; b) H. Zhu, J. Fan, J. Du, X. Peng, *Acc. Chem. Res.* **2016**, *49*, 2115; c) S. Guo, Y. Sun, X. Geng, R. Yang, L. Xiao, L. Qu, Z. Li, *J. Mater. Chem. B* **2020**, *8*, 736.
6. a) W. Liu, C. Li, Y. Ren, X. Sun, W. Pan, Y. Li, J. Wang, W. Wang, *J. Mater. Chem. B* **2016**, *4*, 5772; b) H. Li, Z. Kang, Y. Liu, S.-T. Lee, *J. Mater. Chem.* **2012**, *22*, 24230; c) S. Y. Lim, W. Shen, Z. Gao, *Chem Soc Rev* **2015**, *44*, 362; d) S. N. Baker, G. A. Baker, *Angew. Chem. Int. Ed.* **2010**, *49*, 6726; e) X. Xu, R. Ray, Y. Gu, H. J. Ploehn, L. Gearheart, K. Raker, W. A. Scrivens, *J. Am. Chem. Soc.* **2004**, *126*, 12736; f) T. A. Swift, M. Duchi, S. A. Hill, D. Benito-Alifonso, R. L. Harniman, S. Sheikh, S. A. Davis, A. M. Seddon, H. M. Whitney, M. C. Galan, T. A. A. Oliver, *Nanoscale* **2018**, *10*, 13908; g) S. A. Hill, D. Benito-Alifonso, S. A. Davis, D. J. Morgan, M. Berry, M. C. Galan, *Sci. Rep.* **2018**, *8*; h) S. Hill, M. C. Galan, *Beilstein J. Org. Chem.* **2017**, *13*, 675; i) S. A. Hill, D. Benito-Alifonso, D. J. Morgan, S. A. Davis, M. Berry, M. C. Galan, *Nanoscale* **2016**, *8*, 18630.
7. a) S. Y. Lim, W. Shen, Z. Q. Gao, *Chem. Soc. Rev.* **2015**, *44*, 362; b) P. Miao, K. Han, Y. G. Tang, B. D. Wang, T. Lin, W. B. Cheng, *Nanoscale* **2015**, *7*, 1586; c) S. N. Baker, G. A. Baker, *Angew. Chem. Int. Edit* **2010**, *49*, 6726; d) N. L. Teradal, R. Jelinek, *Adv. Healthc. Mater.* **2017**, *6*; e) P. Miao, K. Han, Y. Tang, B. Wang, T. Lin, W. Cheng, *Nanoscale* **2015**, *7*, 1586.
8. a) D. Zhong, Y. Zhuo, Y. Feng, X. Yang, *Biosens. Bioelectron.* **2015**, *74*, 546; b) F. Lin, C. Li, Z. Chen, *Front. Microbiol.* **2018**, *9*, 2697; c) C. I. Weng, H. T. Chang, C. H. Lin, Y. W. Shen, B. Unnikrishnan, Y. J. Li, C. C. Huang, *Biosens. Bioelectron.* **2015**, *68*, 1–6, <https://doi.org/10.1016/j.bios.2014.12.028> d) F. M. Lin, Y. W. Bao, F. G. Wu, *C-J Carbon Res.* **2019**, *5*; e) H. Wang, F. Lu, C. Ma, Y. Ma, M. Zhang, B. Wang, Y. Zhang, Y. Liu, H. Huang, Z. Kang, *J. Mater. Chem. B* **2021**, *9*, 125; f) H. Li, J. Huang, Y. Song, M. Zhang, H. Wang, F. Lu, H. Huang, Y. Liu, X. Dai, Z. Gu, Z. Yang, R. Zhou, Z. Kang, *ACS Appl. Mater. Interf.* **2018**, *10*, 26936; g) S. Mandal, S. R. Prasad, D. Mandal, P. Das, *ACS Appl. Mater. Interf.* **2019**, *11*, 33273; h) X. Dong, W. Liang, M. J. Mezzani, Y. P. Sun, L. Yang, *Theranostics* **2020**, *10*, 671.
9. H. Zhu, W. Lao, Q. Chen, Q. Zhang, H. Chen, *Int. J. Clin. Exp. Med.* **2015**, *8*, 3651.
10. a) D. Benito-Alifonso, B. Richichi, V. Baldoneschi, M. Berry, M. Fragai, G. Salerno, M. C. Galan, C. Nativi, *ACS Omega* **2018**, *3*, 9822; b) D. Benito-Alifonso, S. Tremel, B. Hou, H. Lockyear, J. Mantell, D. J. Fermin, P. Verkade, M. Berry, M. C. Galan, *Angew. Chem. Int. Ed.* **2014**, *53*, 810; c) R. Levy, U. Shaheen, Y. Cesbron, V. See, *Nano Rev.* **2010**, *1*; d) M. Lundqvist, J. Stigler, G. Elia, I. Lynch, T. Cedervall, K. A. Dawson, *Proc. Natl. Acad. Sci.* **2008**, *105*, 14265; e) D. Bartczak, O. L. Muskens, S. Nitti, T. Sanchez-Elsner, T. M. Millar, A. G. Kanaras, *Small* **2012**, *8*, 122; f) H. Yuan, A. M. Fales, T. Vo-Dinh, *J. Am. Chem. Soc.* **2012**, *134*, 11358.
11. S. A. Hill, S. Sheikh, Q. Y. Zhang, L. S. Ballesteros, A. Herman, S. A. Davis, D. J. Morgan, M. Berry, D. Benito-Alifonso, M. C. Galan, *Nanoscale Adv.* **2019**, *1*, 2840.
12. a) A. Zhu, J. B. Huang, A. Clark, R. Romero, H. R. Petty, *Carbohydr. Res.* **2007**, *342*, 2745; b) A. Bhattacharjee, Y. Hrynets, M. Betti, *J. Agr. Food Chem.* **2017**, *65*, 4642.
13. Y. Hrynets, A. Bhattacharjee, M. Ndagijimana, D. J. Hincapie Martinez, M. Betti, *J. Agric. Food Chem.* **2016**, *64*, 3266.
14. K. Cremin, B. A. Jones, J. Teahan, G. N. Meloni, D. Perry, C. Zerfass, M. Asally, O. S. Soyer, P. R. Unwin, *Anal. Chem.* **2020**, *92*, 16024.
15. Q. Sun, W. Margolin, *J. Bacteriol.* **1998**, *180*, 2050.
16. A. Bhattacharjee, Y. Hrynets, M. Betti, *Food. Chem.* **2019**, *271*, 354.
17. Note that the internal bacteria temperature could not be determined and is likely to be slightly higher than that measured in the bacterial suspension.
18. F. C. Fang, *mBio.* **2011**, *2*.
19. L. Zhang, C. Zhu, R. Huang, Y. Ding, C. Ruan, X. C. Shen, *Front. Chem.* **2021**, *9*, 630969.
20. a) M. Kuroda, H. Kuroda, T. Oshima, F. Takeuchi, H. Mori, K. Hiramatsu, *Mol. Microbiol.* **2003**, *49*, 807; b) S. Utaida, P. M. Dunman, D. Macapagal, E. Murphy, S. J. Projan, V. K. Singh, R. K. Jayaswal, B. J. Wilkinson, *Microbiology* **2003**, *149*, 2719; c) F. McAleese, S. W. Wu, K. Sieradzki, P. Dunman, E. Murphy, S. Projan, A. Tomasz, *J. Bacteriol.* **2006**, *188*, 1120; d) A. Muthaiyan, J. A. Silverman, R. K. Jayaswal, B. J. Wilkinson, *Antimicrob. Agents Chemother.* **2008**, *52*, 980.
21. a) M. J. Mezzani, X. Dong, L. Zhu, L. P. Jones, G. E. LeCroy, F. Yang, S. Wang, P. Wang, Y. Zhao, L. Yang, R. A. Tripp, Y. P. Sun, *ACS Appl Mater Interfaces* **2016**, *8*, 10761; b) R. Jijie, A. Barras, J. Bouckaert, N. Dumitrascu, S. Szunerits, R. Boukherroub, *Colloids Surf. B Biointerf.* **2018**, *170*, 347.
22. a) N. Sattarahmady, M. Rezaie-Yazdi, G. H. Tondro, N. Akbari, *J. Photochem. Photobiol. B* **2017**, *166*, 323; b) R. Knoblauch, C. D. Geddes, *Materials* **2020**, *13*.
23. J. K. Eng, A. L. McCormack, J. R. Yates, *J. Am. Soc. Mass Spectrom.* **1994**, *5*, 976.
24. RStudio Team (2020). *RStudio: Integrated Development for R*. RStudio, PBC, Boston, MA, <http://www.rstudio.com/>
25. H. Mi, D. Ebert, A. Muruganujan, C. Mills, L.-P. Albou, T. Mushayamaha, P. D. Thomas. *Nucl. Acids Res.* **2021**, *49*, D394.

**How to cite this article:** J. Samphire, Y. Takebayashi, S. A. Hill, N. Hill, K. J. Heesom, P. A. Lewis, D. Alibhai, E. C. Bragginton, J. Dorh, N. Dorh, J. Spencer, M. C. Galan. *Nano Select.* **2021**, *1*. <https://doi.org/10.1002/nano.202100183>